1-1-2013

Thermoelectric properties of Ca3Co4O9 and Ca2.8Bi0.2Co4O9 thin films in their island formation mode

Priyanka Jood
University of Wollongong, pj991@uow.edu.au

Germanas Peleckis
University of Wollongong, peleckis@uow.edu.au

Xiaolin Wang
University of Wollongong, xiaolin@uow.edu.au

S X. Dou
University of Wollongong, shi@uow.edu.au

Thermoelectric properties of Ca3Co4O9 and Ca2.8Bi0.2Co4O9 thin films in their island formation mode

Abstract

Ca3Co4O9 and Ca2.8Bi 0.2Co4O9 thin films were fabricated on LaAlO3 (LAO) substrate using pulsed laser deposition technique and were studied for their thermoelectric (TE) properties in Stranski-Krastanov mode for the first time. The thin films consisted of 3D clusters/islands on a 14-nm thick 2D layer with cluster density being higher for Ca 2.8Bi0.2Co4O9 thin films. The clusters also represent areas of dislocation and therefore act as carrier scattering centers, which leads to a temperature-activated type conductivity. Seebeck coefficient as high as 136 and 163 u V/K was measured for the Ca 3Co4O9 and Ca2.8Bi 0.2Co4O9 thin films, respectively, which is among the highest reported values for this system. The 3D island formation was also found to be useful in reducing the thermal conductivity of the thin film/ substrate system by increased phonon scattering. This work shows that the island formation in thin films can be utilized as a means of enhancing TE properties of a thin film system, however, a detailed work including optimization of the film thickness and cluster/inland density is required.

Keywords

formation, mode, island, properties, their, thermoelectric, films, thin, 2co4o9, 8bi0, ca2, ca3co4o9

Disciplines

Engineering | Physical Sciences and Mathematics

Publication Details

Jood, P., Peleckis, G., Wang, X. & Dou, S. X. (2013). Thermoelectric properties of Ca3Co4O9 and Ca2.8Bi0.2Co4O9 thin films in their island formation mode. Journal of Materials Research, 28 (14), 1932-1939.

Thermoelectric properties of $Ca_3Co_4O_9$ and $Ca_{2.8}Bi_{0.2}Co_4O_9$ thin films in their island formation mode

Priyanka Jood,[a] Germanas Peleckis, Xiaolin Wang, and Shi Xue Dou
Institute for Superconducting and Electronic Materials, University of Wollongong, Wollongong, New South Wales 2519, Australia

(Received 5 February 2013; accepted 15 May 2013)

$Ca_3Co_4O_9$ and $Ca_{2.8}Bi_{0.2}Co_4O_9$ thin films were fabricated on $LaAlO_3$ (LAO) substrate using pulsed laser deposition technique and were studied for their thermoelectric (TE) properties in Stranski–Krastanov mode for the first time. The thin films consisted of 3D clusters/islands on a ~14-nm thick 2D layer with cluster density being higher for $Ca_{2.8}Bi_{0.2}Co_4O_9$ thin films. The clusters also represent areas of dislocation and therefore act as carrier scattering centers, which leads to a temperature-activated type conductivity. Seebeck coefficient as high as 136 and 163 μ V/K was measured for the $Ca_3Co_4O_9$ and $Ca_{2.8}Bi_{0.2}Co_4O_9$ thin films, respectively, which is among the highest reported values for this system. The 3D island formation was also found to be useful in reducing the thermal conductivity of the thin film/substrate system by increased phonon scattering. This work shows that the island formation in thin films can be utilized as a means of enhancing TE properties of a thin film system, however, a detailed work including optimization of the film thickness and cluster/inland density is required.

I. INTRODUCTION

Thermoelectric (TE) phenomena involve the conversion between waste heat and electrical energy and have therefore attracted much interest in the research society owing to its vast applications. The efficiency of a TE material is judged by its figure of merit, $ZT = \alpha^2\sigma T/\kappa$, where α is the Seebeck coefficient, σ is the electrical conductivity, κ is the thermal conductivity, and T is the absolute temperature. Electrical power generation from waste heat, e.g., in cars, aircrafts, and power plants, requires high stability TE materials with high figures of merit ZT at temperatures above 600 K, and therefore, oxide materials are promising in this regard due to their nontoxicity, high oxidation resistance, and thermal stability at high temperatures. $Ca_3Co_4O_9$ is among the most promising *p*-type oxide materials for high temperature TE applications, with the figure-of-merit (ZT) obtained for a single crystal reaching as high as 0.83 at 1000 K.[1] Although many advanced applications require large-size $Ca_3Co_4O_9$ single crystals, they are difficult to fabricate owing to the strong anisotropy in the crystal growth and electrical properties. Owing to this fact, a large amount of research has been carried out on improving the TE properties of randomly oriented polycrystalline $Ca_3Co_4O_9$ ceramics, but with very limited improvement.[2–5] Therefore, several efforts have been made to improve the texture of $Ca_3Co_4O_9$ ceramic by various methods, such as spark plasma sintering,[6] magnetic alignment,[7] and hot-forging processes,[8] owing to a general belief that the grain boundaries negatively affect the electrical conductivity and hence the TE properties of this system. The epitaxial growth and *c*-axis-oriented films fabricated using the pulsed laser deposition (PLD),[9,10] radio-frequency magnetron sputtering,[11] and the topotactic ion exchange method[12] have proven to be successful in improving the TE properties of this system. The thin film approach not only holds the potential of reducing the thermal conductivity of the system through lattice mismatch and the introduction of various scattering centers in the film but can also result in the enhancement of thermopower through structures such as superlattices and quantum wells.[13]

A large power factor, $\alpha^2\sigma$ enhancement was reported for PbTe and PbSe thin films comprising of 3-dimensional island formations. A large electrical conductivity, σ, and carrier mobility, μ, in these thin film systems were explained by the self-ordering of islands in the growing thin film. These studies inspired us to study the island mode of thin film growth and the factors influencing the density, size, and distribution of these islands in $Ca_3Co_4O_9$ thin film system. The goal of the present work is to study the TE properties of $Ca_3Co_4O_9$ ultrathin film in their island growth mode. In this study, we used the PLD technique to deposit $Ca_3Co_4O_9$ and $Ca_{2.8}Bi_{0.2}Co_4O_9$ thin films on a $LaAlO_3$ (LAO) substrate. Bismuth was chosen as a dopant because Bi substitution has been proven to be effective in increasing thermopower (α) while maintaining electrical conductivity (σ) in the bulk counterpart of this system,[3–5] as well as in single crystals[14] and thin films.[15,16]

[a]Address all correspondence to this author.
e-mail: joodpriyanka@gmail.com, pj991@uowmail.edu.au
DOI: 10.1557/jmr.2013.163

II. EXPERIMENTAL

$Ca_3Co_4O_9$ and $Ca_{2.8}Bi_{0.2}Co_4O_9$ (denoted as CCO and CB02 respectively) thin films were prepared on a (001)-oriented perovskite-based substrate, $LaAlO_3$ (LAO), at substrate temperatures between 550 and 750 °C and 10 Pa oxygen pressure with a Nd: YAG laser (Lab-170, $\lambda = 355$ nm). The laser energy density and repetition rate were fixed at 0.15 J/cm^2/pulse and 10 Hz, respectively. The ceramic targets were synthesized through the solid state reaction method as follows: The oxide powders, namely, $CaCO_3$ (≥99%, Sigma Aldrich, Castle Hill, NSW, Australia), Co_3O_4 (99.995%, Sigma Aldrich), and Bi_2O_3 (≥99.5%, Sigma Aldrich), in their required ratios were mixed together in a planetary ball mill for 12 h and then calcined at 700 °C/12 h. After cooling down, this powder mixture was again ball milled for 5 h and calcined again at 700 °C/20 h. The powder was then compacted into pellets in the form of 1-inch diameter disks under a pressure of 40 MPa and then sintered at a temperature of 750 °C for 20 h, with the sintering procedure repeated twice.

The phase purity of the final target samples as well as that of the thin films was detected by x-ray diffraction (XRD) analysis by means of a GBC MMA diffractometer with a Cu K_α radiation source ($\lambda = 0.154$ nm). The surface roughness of the thin films was characterized by an atomic force microscope (AFM; Asylum Research MFP-3D SA, Santa Barbara, CA). The surface topographies of the thin films were examined by using a scanning electron microscope (SEM; JEOL7500 FA, New South Wales, Australia) and the SEM images were analyzed using ImageJ software. The TE properties of $Ca_3Co_4O_9$/LAO and $Ca_{2.8}Bi_{0.2}Co_4O_9$/LAO were determined using a physical properties measurement system (PPMS, Quantum Design, San Diego, CA) configured with the thermal transport option (TTO) in zero magnetic field from 50 to 350 K. The sample preparation for PPMS involved attaching four leads to the sample with a conducting epoxy.

III. RESULTS AND DISCUSSION

A. Fabrication and characterization

Substrate temperature is known to be a critical parameter in the thin film fabrication, and therefore, its optimization is necessary.[17,18] Initially, $Ca_3Co_4O_9$ thin film was fabricated on the LAO substrate at three different substrate temperatures, i.e., 550, 600, and 750 °C. All the parameters except the substrate temperature were kept constant. For the thin film deposited at 550 °C, the crystallinity was found to be quite poor. This can be attributed to the PLD kinetics, where high substrate temperature can provide sufficient surface diffusion to allow surface atoms to migrate toward thermodynamically stable sites and crystallize.[10] Therefore, increasing the substrate temperature to 600 °C improved the crystallinity of the film, as seen in the XRD pattern [Fig. 1(a)], which shows diffraction peaks corresponding to only (001) $Ca_3Co_4O_9$ film reflections or reflections from the substrate. The XRD pattern therefore shows a dominant *c*-axis alignment with no evidence of the secondary phase in this film. Increasing the substrate temperature further to 750 °C partly decomposed the $Ca_3Co_4O_9$ phase into $Ca_3Co_2O_6$ phase,[19] with reflections marked in the XRD pattern [Fig. 1(b)].

Several kinds of growth modes and characteristic structures can be observed during the deposition of atoms on a flat substrate.[20] A layer-by-layer or an epitaxial growth mode is called the Frank–van der Merwe mode (FM). However, sometimes the FM structure is found to exhibit undulations in the thickness, which is an indication of the uniform film being unstable. This leads to an eventual breakup of the FM film structure into a Stranski–Krastanov mode (SK) or Volmer–Weber mode (VW). The SK growth method is observed in our $Ca_3Co_4O_9$ thin film. It is described as an initial 2D growth of a few monolayers with grains oriented in a (001) orientation [Fig. 2(a)], followed by 3D cluster/island growth on these monolayers [Fig. 2(b)]. In the literature, different kinds of growth

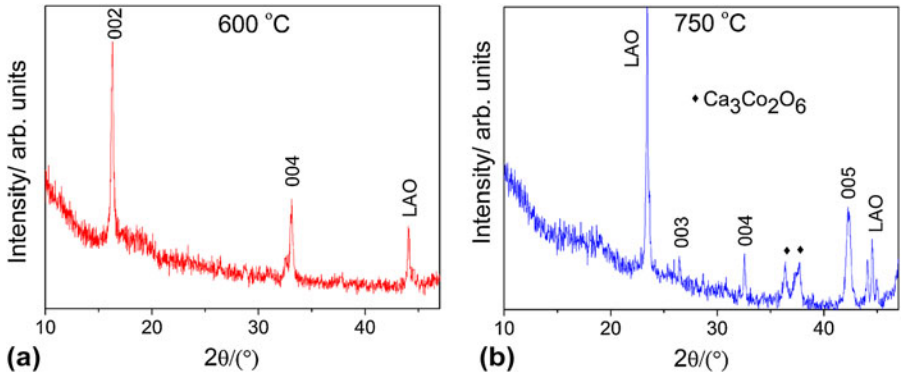

FIG. 1. XRD patterns of pure $Ca_3Co_4O_9$ (CCO) thin films deposited on LAO substrate at a substrate temperature of (a) 600 °C and (b) 750 °C.

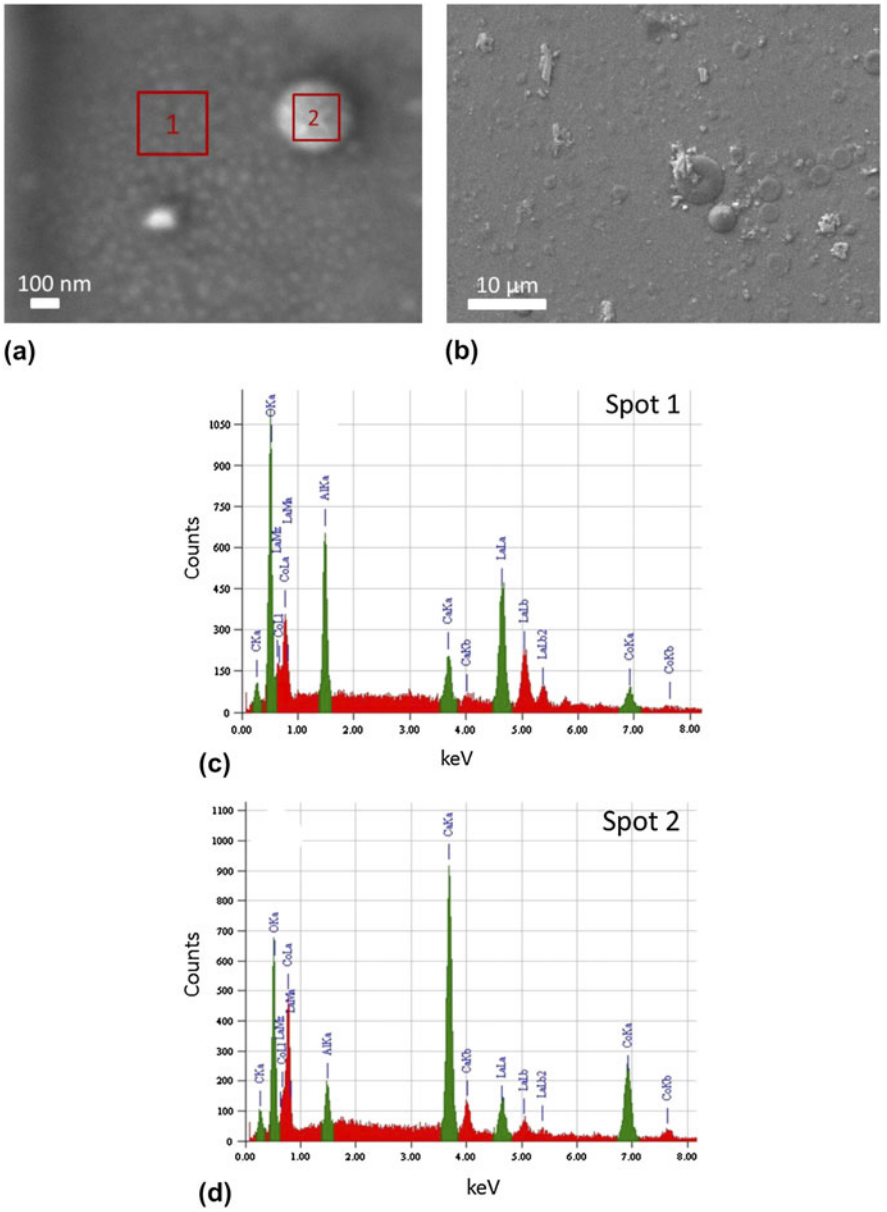

FIG. 2. SEM micrographs of the surface of the thin $Ca_3Co_4O_9$ film showing (a) the initial 2D growth of monolayers with grains aligned in a (001) orientation, and (b) lower magnification image of the film showing the 3D cluster growth. (c) and (d) are the EDS spectra collected from Spot 1 and Spot 2 of (a), respectively.

modes such as VW[10] and columnar[21] have been achieved for the PLD deposited $Ca_3Co_4O_9$ system apart from the epitaxial growth.[22]

AFM images of the as-grown $Ca_3Co_4O_9$ thin film also confirm the SK growth structure. A height profile of the 2D thin film was taken over the location indicated in the AFM image in Fig. 3(a). A 1.4-µm long line profile in Fig 3(b) shows that the thickness of the 2D thin film is ~14 nm, and the clusters are an average of ~90 nm high. Energy dispersive spectroscopy (EDS) spectra were collected from different spots on the thin film, and it was observed that the clusters were comprised of Ca_xCoO_2 phase along with excess Ca. For example, the EDS spectra in Figs. 2(c) and 2(d) were taken from the thin film and the cluster, respectively, and clearly exhibit the difference in the Ca content between the two spots. A similar result was reported by Cieniek et al.[21] in their study of (Co, Ca)O PLD thin films, as they also observed Ca rich droplets on their thin films, the origin of which is not very clear. From the quantitative EDS data, the cation ratio of the 2D part of the thin film (Spot 1) was determined to be Ca:Co = 3:4.1, which shows that the stoichiometry in the thin film is maintained. It is stated in the literature[10] that during the PLD synthesis, the Ca_xCoO_2 structure

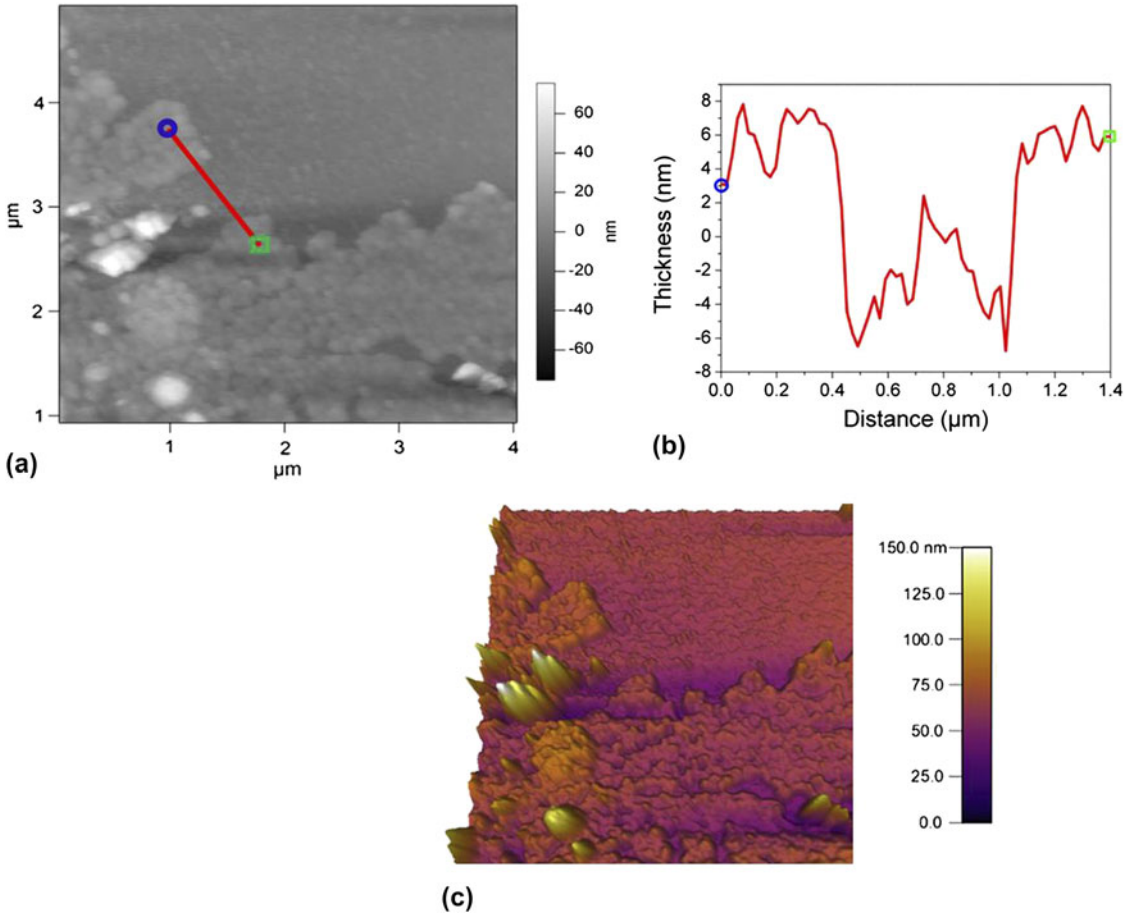

FIG. 3. (a) AFM images of the $Ca_3Co_4O_9$ thin film on LAO substrate deposited at a substrate temperature of 600 °C. (b) Height profile of the 2D thin film taken over the location indicated by the red line in the AFM image in (a). (c) Three dimensional AFM image of the thin film.

forms first, particularly at the boundaries of nuclei with high defect density. The Ca to Co cationic ratio from Spot 2 (clusters) is determined to be 1.16:1. Although, the elemental composition of Ca_xCoO_2 lies between $0.26 \leq x \leq 0.5$,[10] it is also known that excess Ca exists when Ca_xCoO_2 phase is formed on the substrate. This could explain the excess Ca in the clusters. However, if given enough ripening time during the coalescence process of the nuclei, a well-aligned CCO thin film can be formed. In a different process, Ca_xCoO_2 can also combine with ambient Ca and oxygen and transform into the CCO structure, again giving us a well-textured CCO thin film. Following the above argument, the clusters can be thought of as the initial formation of the CCO structure, and therefore, they consist of Ca_xCoO_2 phase along with excess Ca as indicated by EDS analysis.

$Ca_3Co_4O_9$ thin film with 2 at.% Bi doping was also deposited on the LAO substrate. The SEM micrographs in Fig. 4 show the surface morphology of the $Ca_{2.8}Bi_{0.2}Co_4O_9$ thin film. Compared to the pure $Ca_3Co_4O_9$ thin film [Figs. 2(a) and 2(b)], Bi doping not only results in increased grain size [see Fig. 4(a)] but also increases the cluster density in the film [see Fig. 4(b)]. The XRD pattern (Fig. 5) shows the decrease in the peak intensity as well as the broadening of the peaks due to the Bi doping. This deterioration of film crystallinity can be a result of the high cluster density in the $Ca_{2.8}Bi_{0.2}Co_4O_9$ thin film. The cluster size, on the other hand, is observed to be much smaller than for the $Ca_3Co_4O_9$ thin film. Fig. 6 illustrates the average dimensions of the largest clusters observed in both films, along with the variation in film thickness as observed from the AFM and SEM analyses. The average diameter and the average height of the largest cluster for $Ca_{2.8}Bi_{0.2}Co_4O_9$ are found to be ~70% and 22% lower than the ones observed for the $Ca_3Co_4O_9$ thin film, respectively. No apparent change was detected in the thickness of the 2D monolayers in both kinds of films, which was observed to be ~14 nm. As both thin films were deposited under the exact same conditions, as well as for the same time, therefore, the difference in the morphology can be considered to be due to the presence of Bi in the system. It appears that Bi doping reduces the amplitude of the undulations and, hence, restricts the ripening of the clusters. Therefore, the merging of the smaller clusters into the larger

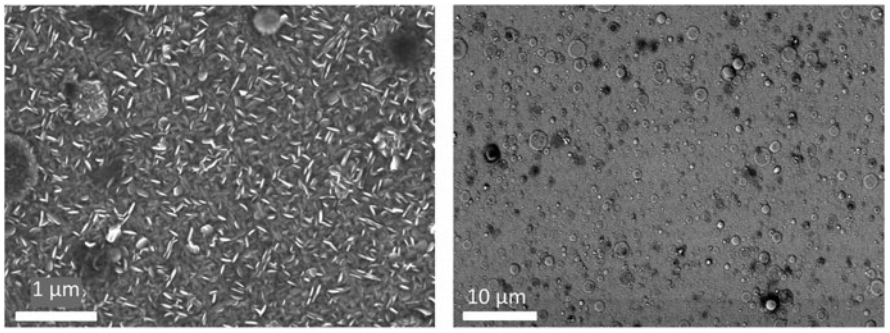

FIG. 4. (a) High and (b) low magnification SEM micrographs of the surface of $Ca_{2.8}Bi_{0.2}Co_4O_9$ thin film deposited on LAO substrate, illustrating the grain size and the cluster density in the film.

ones is impeded, and thus, the process does not allow the average cluster size to increase.[20] This argument explains the large number of relatively small clusters observed in $Ca_{2.8}Bi_{0.2}Co_4O_9$ thin films. This kind of incomplete cluster coalescence also leads to pinhole formation[23,24] which can be seen as the dark spots in Fig. 4. These pinholes (~50 nm to 2 μm in size) are expected to further reduce the thermal conductivity due to increased phonon scattering.

B. TE properties of CCO and CB02 thin films

Figure 7(a) shows the electrical transport and Seebeck coefficient for the undoped and Bi-doped samples. The trend in the electrical conductivity in our films indicates semiconductor-type transport in the temperature range studied. This behavior is very different from the one observed in the literature,[12] which is metallic for the temperatures between ~100 and 400 K. Also, our values for σ_{350K} are 705 and 388/Ω/m for $Ca_3Co_4O_9$ and $Ca_{2.8}Bi_{0.2}Co_4O_9$ thin films, respectively, which are lower than earlier reported values,[25] the basic reason for which can be suggested as the island formation of the film. Now, as the effective 2D film thickness is very low in our case, therefore, a contribution of electrical conduction from the clusters is also expected and cannot be neglected. These clusters, as discussed in Sec. III. A, are considered to consist of the Ca_xCoO_2 phase, which has higher electrical resistivity than $Ca_3Co_4O_9$ phase, although both have layered structures.[26,27] The clusters present in our thin films also represent areas of dislocation and incomplete nucleation and, hence, might act as carrier-scattering centers decreasing carrier mobility. We propose that the conduction in our thin films takes place through a temperature-activated hopping mechanism in the temperature range measured. During the conduction process, the holes are eventually trapped at structural defects, which are the clusters in our case, and the transport continues as a tunneling from one defect to another, causing the unusual transport phenomena.[28]

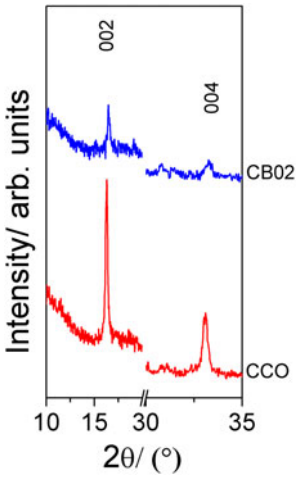

FIG. 5. XRD patterns showing two most prominent peaks, (002) and (004), of $Ca_3Co_4O_9$ (CCO) and $Ca_{2.8}Bi_{0.2}Co_4O_9$ (CB02) thin films.

Another point to note is that unlike the earlier reported work, Bi doped film is more resistive than the pure $Ca_3Co_4O_9$ thin film [Fig 7(a)]. It is known that with Bi doping, the effective carrier concentration decreases due to the Bi^{+3} substitution for divalent Ca^{+2} in the (Ca_2CoO_3) layers, which inject electrons into the conductive (CoO_2) layer.[15] Therefore, the increase in conductivity due to Bi doping has been reported to take place due to the improvement in the charge carrier mobility and not through increased carrier concentration.[3] However, this does not seem to be happening in our case. This can be related to the increase in the cluster density as a result of Bi doping. It was shown that the trapping rate of the holes is directly proportional to the concentration of trapping sites (in our case, clusters) and the radius of trapping sites.[28] As the increase in cluster density with Bi doping is much higher than the reduction in the cluster radius, therefore, we can assume that the increase in resistivity is mainly caused by the larger number of clusters, which consequently increases the number of defect sites and dislocations in the structure of the film.

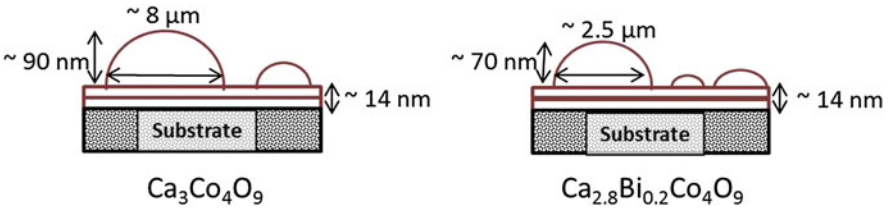

FIG. 6. A Schematic illustration of the differences in surface morphology between the two studied thin film families.

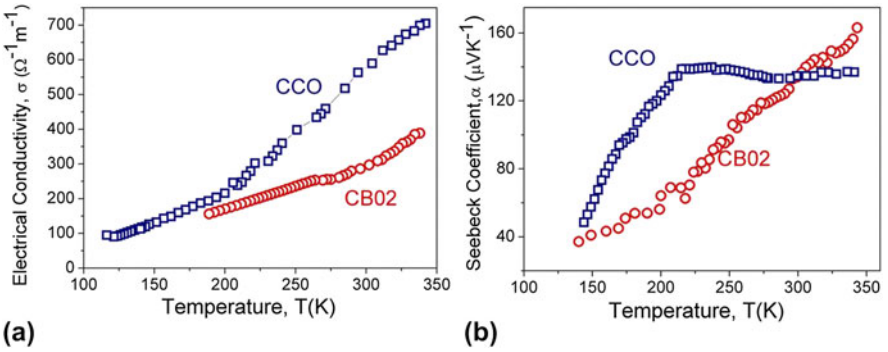

FIG. 7. Temperature dependence of (a) electrical conductivity (σ) and (b) Seebeck coefficient (α) for $Ca_3Co_4O_9$ and $Ca_{2.8}Bi_{0.2}Co_4O_9$ thin films.

The room temperature Seebeck coefficient [Fig. 7(b)] for our $Ca_3Co_4O_9$ and $Ca_{2.8}Bi_{0.2}Co_4O_9$ thin films is found to be 136 and 163 µ V/K, respectively, which is among the largest α_{300K} reported for $Ca_3Co_4O_9$ thin films.[16] Such a high Seebeck coefficient compensates for the lower electrical conductivity and results in a reasonable power factor of $\alpha^2\sigma_{300K} \approx 0.13 \times 10^{-4}$ W/m/K^2 for CCO and $\alpha^2\sigma_{300K} \approx 0.1 \times 10^{-4}$ W/m/K^2 for CB02 thin film. These values fit well among those reported previously for this system.[12,15] Furthermore, the Seebeck coefficient of CB02 thin film increases almost linearly with increasing temperature. Now, similar to the Drude picture, the Seebeck coefficient of the $Ca_3Co_4O_9$ system can be expressed as $\alpha \approx c_e/n$,[15] where c_e is the electronic specific heat and n is the carrier concentration. As n is known to decrease with Bi doping, the increase in α due to the Bi doping is expected. Also, a large thermopower in our thin films can be explained on the basis of the fact that the Seebeck coefficient for a given carrier density n increases as the scattering parameter increases.[29] The presence of resistive clusters surrounded by defects and dislocations, which are considered as trap sites for holes, can be considered a source of efficient sites for filtering the charge carriers having lowest energies, resulting in a large Seebeck coefficient. Further power factor enhancements could be achieved by tuning the thickness of the thin film. Inhomogeneous thin film consisting of conducting and nonconducting constituents has been observed to exhibit an abrupt increase in electrical conductivity within a narrow thickness range, which is explained by percolation theory by some authors.[30] A sharp growth in carrier mobility and electrical conductivity is expected during the transition from island mode to continuous thin film. A detailed work constituting the dependence of TE properties on varying thickness of the $Ca_3Co_4O_9$ ultrathin film is ongoing.

The obtained values of thermal conductivity (κ) are measured as a whole parameter (Fig. 8), i.e., the thin film plus the substrate. We see that the major κ contribution in the CCO and CB02 thin films comes from the LAO substrate with $\kappa_{350K} \approx 11.4$ W/m/K. The carrier contribution κ_{carr} toward total κ was calculated using the relation[2]:

$$\kappa_{carr} = \frac{L_0 T}{\rho} \kappa_{carr} = \frac{L_0 T}{\rho} \quad ,$$

where, L_0 is the Lorenz number, whose value is 2.44×10^{-8} W Ω/K^2, T is the temperature in Kelvin, and ρ is the electrical resistivity in Ω-m. The values of carrier thermal conductivity κ_{carr} are calculated to be very low, i.e., less than ~0.005 W/m/K and ~0.003 W/m/K for CCO and CB02, respectively. Even though the κ_{carr} for CB02 is ~30% lower than for CCO, we still observe a lower κ_{total} of ~8.5 W/m/K for CB02/LAO compared with the κ_{total} of ~11.2 W/m/K for CCO/LAO. These figures indicate that the CB02/LAO sample has a significantly larger number of phonon scattering centers as compared with the CCO/LAO thin film. This again can be easily related to the presence of a higher cluster density as well as the presence of pinholes in the CB02 thin film. These figures are quite figurative and to determine the real thermal conductivity of the individual films, a special measurement technique is required which can separate the

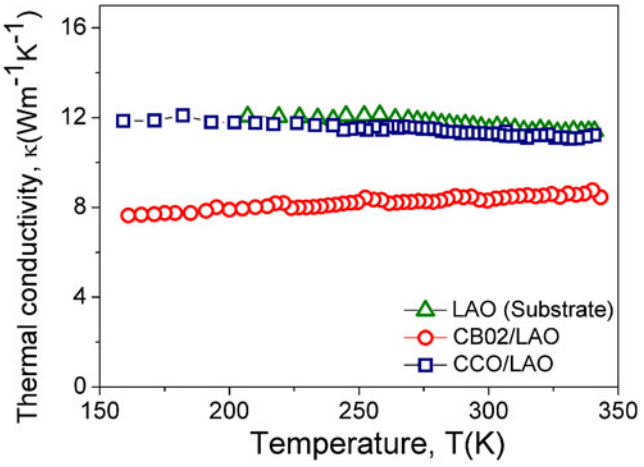

FIG. 8. Temperature dependence of thermal conductivity of the CCO and CBO2 thin films on LAO substrate along with the thermal conductivity of the substrate for comparison.

thermal conductivity contribution of the substrate from that of the actual thin film. This additional information would provide important information on the intrinsic thermoelectrical properties of Ca-349 thin films having a SK formation.

IV. CONCLUSION

In this study, $Ca_3Co_4O_9$ and $Ca_{2.8}Bi_{0.2}Co_4O_9$ thin films were fabricated on LAO substrate using the PLD technique with varying substrate temperatures between 500 and 750 °C, with samples deposited at 600 °C being selected as representatives. The growth mode in our thin films was observed to be SK mode, in which the structure consists of initial 2D thin layers followed by the growth of 3D clusters/islands. The effective film thickness was determined to be ~14 nm for both groups of thin films. Bi-doped samples showed a considerably higher density of clusters as compared with undoped samples. Owing to this cluster growth, a peculiar electrical conductivity trend was observed in our thin films where conductivity increased with temperature in the temperature range studied. We report a very high room temperature Seebeck coefficient for both thin films with values of 136 and 163 μ V/K for CCO and CB02, giving us a considerable high power factor of $\sim 0.13 \times 10^{-4}$ W/m/K^2 for CCO and $\alpha^2\sigma_{300K} \approx 0.1 \times 10^{-4}$ W/m/K^2 for CB02 thin films. We found that the formation of clusters helped in the reduction of thermal conductivity. It is evident that further improvements to the properties of the films are necessary. These can be achieved through a thorough study of the dependence of TE properties on the thickness of the thin film. Structural and TE effects and phenomena observed during the course of this work suggest that detailed microstructure studies and the development of new physical approaches and models are necessary to fully understand the TE conversion potential of this oxide-based material.

ACKNOWLEDGMENTS

G.P. thanks the Australian Research Council for support under Discovery Grant No. DP0 879 714. P.J. thanks the University of Wollongong for providing matching scholarship for her Ph.D. studies. X.W. thanks the Australian Research Council for support under Discovery Grant No. DP1 094 073.

REFERENCES

1. M. Shikano and R. Funahashi: Electrical and thermal properties of single-crystalline $(Ca_2CoO_3)_{0.7}CoO_2$ with a $Ca_3Co_4O_9$ structure. *Appl. Phys. Lett.* **82**, 1851 (2003).
2. W. Yang, S. Yu, C. Jinguang, W. Xianjie, and S. Wenhui: The thermal-transport properties of the $Ca_{3-x}Ag_xCo_4O_9$ system ($0 \le x \le 0.3$). *J. Phys. Condens. Matter* **19**, 356216 (2007).
3. G. Xu, R. Funahashi, M. Shikano, I. Matsubara, and Y. Zhou: Thermoelectric properties of the Bi- and Na-substituted $Ca_3Co_4O_9$ system. *Appl. Phys. Lett.* **80**, 3760 (2002).
4. M. Mikami, N. Ando, E. Guilmeau, and R. Funahashi: Effect of Bi substitution on microstructure and thermoelectric properties of polycrystalline $[Ca_2CoO_3]_pCoO_2$. *Jpn. J. Appl. Phys., Part 1* **45**, 4152 (2006).
5. Y. Liu, Y. Lin, L. Jiang, C-W. Nan, and Z. Shen: Thermoelectric properties of Bi^{3+} substituted Co-based misfit-layered oxides. *J. Electroceram.* **21**, 748 (2008).
6. Y. Zhang, J. Zhang, and Q. Lu: Synthesis of highly textured $Ca_3Co_4O_9$ ceramics by spark plasma sintering. *Ceram. Int.* **33**, 1305 (2007).
7. Y. Zhou, I. Matsubara, S. Horii, T. Takeuchi, R. Funahashi, M. Shikano, J-I. Shimoyama, K. Kishio, W. Shin, N. Izu, and N. Murayama: Thermoelectric properties of highly grain-aligned and densified Co-based oxide ceramics. *J. Appl. Phys.* **93**, 2653 (2003).
8. M. Prevel, S. Lemonnier, Y. Klein, S. Hebert, D. Chateigner, B. Ouladdiaf, and J.G. Noudem: Textured $Ca_3Co_4O_9$ thermoelectric oxides by thermoforging process. *J. Appl. Phys.* **98**, 093706 (2005).
9. Q. Qiao, A. Gulec, T. Paulauskas, S. Kolesnik, B. Dabrowski, M. Ozdemir, C. Boyraz, D. Mazumdar, A. Gupta, and R.F. Klie: Effect of substrate on the atomic structure and physical properties of thermoelectric $Ca_3Co_4O_9$ thin films. *J. Phys. Condens. Matter* **23**, 305005 (2011).
10. T. Sun, H.H. Hng, Q. Yan, and J. Ma: Effects of pulsed laser deposition conditions on the microstructure of $Ca_3Co_4O_9$ thin films. *J. Electron. Mater.* **39**, 1611 (2010).
11. A. Sakai, T. Kanno, S. Yotsushashi, A. Odagawa, and H. Adachi: Control of epitaxial growth orientation and anisotropic thermoelectric properties of misfit-type $Ca_3Co_4O_9$ thin films. *Jpn. J. Appl. Phys.* **44**, L966 (2005).
12. K. Sugiura, H. Ohta, K. Nomura, M. Hirano, H. Hosono, and K. Koumoto: High electrical conductivity of layered cobalt oxide $Ca_3Co_4O_9$ epitaxial films grown by topotactic ion-exchange method. *Appl. Phys. Lett.* **89**, 032111 (2006).
13. L.D. Hicks and M.S. Dresselhaus: Effect of quantum-well structures on the thermoelectric figure of merit. *Phys. Rev. B* **47**, 12727 (1993).
14. M. Mikami, K. Chong, Y. Miyazaki, T. Kajitani, T. Inoue, S. Sodeoka, and R. Funahashi: Bi-substitution effects on crystal structure and thermoelectric properties of $Ca_3Co_4O_9$ single crystals. *Jpn. J. Appl. Phys.* **45**, 4131 (2006).
15. T. Sun, H.H. Hng, Q.Y. Yan, and J. Ma: Enhanced high temperature thermoelectric properties of Bi-doped c-axis oriented $Ca_3Co_4O_9$ thin films by pulsed laser deposition. *J. Appl. Phys.* **108**, 083709 (2010).

16. Y. Zhou, I. Matsubara, W. Shin, N. Izu, and N. Murayama: Effect of grain size on electric resistivity and thermopower of $(Ca_{2.6}Bi_{0.4})Co_4O_9$ thin films. *J. Appl. Phys.* **95**, 625 (2004).
17. M. Ohtake, Y. Nukaga, F. Kirino, and M. Futamoto: Effects of substrate temperature and Cu underlayer thickness on the formation of $SmCo_5$(0001) epitaxial thin films. *J. Appl. Phys.* **107**, 09A706 (2010).
18. R. Sathyamoorthy, S.K. Narayandaas, and D. Mangalaraj: Effect of substrate temperature on the structure and optical properties of CdTe thin film. *Sol. Energy Mater. Sol. Cells* **76**, 339 (2003).
19. Y.F. Zhang, J.X. Zhang, Q.M. Lu, and Q.Y. Zhang: Synthesis and characterization of $Ca_3Co_4O_9$ nanoparticles by citrate sol-gel method. *Mater. Lett.* **60**, 2443 (2006).
20. G.H. Gilmer, H. Huang, and C. Roland: Thin film deposition: Fundamentals and modeling. *Comp. Mater. Sci.* **12**, 354 (1998).
21. L. Cieniek and S. Kac: Influence of Ca content on the structure and properties of (Co, Ca)O thin films deposited by PLD technique. *Acta Phys. Pol. A* **117**, 803 (2010).
22. Y.F. Hu, W.D. Si, E. Sutter, and Q. Li: In situ growth of c-axis oriented $Ca_3Co_4O_9$ thin films on Si (100). *Appl. Phys. Lett.* **86**, 082103 (2005).
23. C.C. Chang, X.D. Wu, R. Ramesh, X.X. Xi, T.S. Ravi, T. Venkatesan, D.M. Hwang, R.E. Muenchausen, S. Foltyn, and N.S. Nogar: Origin of surface roughness for c-axis oriented Y-Ba-Cu-O superconducting films. *Appl. Phys. Lett.* **57**, 1814 (1990).
24. M.A. Hafez, K.A. Elamrawi, and H.E. Elsayed-Ali: Pulsed laser deposition of InP thin films on sapphire(1 0 0 0) and GaAs(1 0 0). *Appl. Surf. Sci.* **233**, 42 (2004).
25. H. Ohta, K. Sugiura, and K. Koumoto: Recent progress in oxide thermoelectric materials: *p*-type $Ca_3Co_4O_9$ and *n*-type $SrTiO_3$. *Inorg. Chem.* **47**, 8429 (2008).
26. T. Sun, J. Ma, Q.Y. Yan, Y.Z. Huang, J.L. Wang, and H.H. Hng: Influence of pulsed laser deposition rate on the microstructure and thermoelectric properties of $Ca_3Co_4O_9$ thin films. *J. Cryst. Growth* **311**, 4123 (2009).
27. T. Kanno, S. Yotsuhashi, and H. Adachi: Anisotropic thermoelectric properties in layered cobaltite A_xCoO_2 (A = Sr and Ca) thin films. *Appl. Phys. Lett.* **85**, 739 (2004).
28. R.C. Hughes: Time-resolved hole transport in a-SiO_2. *Phys. Rev. B* **15**, 2012 (1977).
29. J.P. Heremans, C.M. Thrush, and D.T. Morelli: Thermopower enhancement in PbTe with Pb precipitates. *J. Appl. Phys.* **98**, 063703 (2005).
30. E.I. Rogacheva, O.N. Nashchekina, Y.O. Vekhov, M.S. Dresselhaus, and S.B. Cronin: Effect of thickness on the thermoelectric properties of PbS thin films. *Thin Solid Films* **423**, 115 (2003).